Ferroelectricity in hexagonal $YFeO_3$ film at room temperature*

Zhang Run-Lan(张润兰)[a)b)], Chen Chang-Le(陈长乐)[a)†], Zhang Yun-Jie(张云婕)[a)], Xing Hui(邢 辉)[a)], Dong Xiang-Lei(董祥雷)[a)], and Jin Ke-Xin(金克新)[a)]

[a)] *Shaanxi Key Laboratory of Condensed Matter Structures and Properties, Northwestern Polytechnical University, Xi'an* 710072, *China*
[b)] *College of Chemistry and Chemical Engineering, Xi'an University of Science and Technology, Xi'an* 710054, *China*

(Received 4 June 2014; revised manuscript received 25 August 2014; published online 25 November 2014)

In this paper we report the leakage current, ferroelectric and piezoelectric properties of the $YFeO_3$ film with hexagonal structure, which was fabricated on Si(111) substrate by a simple sol-gel method. The leakage current test shows good characteristics as the leakage current density is 5.4×10^{-6} A/cm^2 under 5 V. The dominant leakage mechanism is found to be an Ohmic behavior at low electric field and space-charge-limited conduction at high electric field region. The *P*–*E* measurements show ferroelectric hysteresis loops with small remnant polarization and coercive field at room temperature. The distinct and switchable domain structures on the nanometer scale are observed by piezoresponse force microscopy, which testifies to the ferroelectricity of the $YFeO_3$ film further.

Keywords: hexagonal $YFeO_3$, multiferroic, ferroelectricity, piezoresponse force microscopy

PACS: 77.55.Nv, 77.84.–s, 68.37.Ps, 73.40.–c **DOI:** 10.1088/1674-1056/24/1/017701

1. Introduction

Multiferroic materials providing both ferroelectric and ferromagnetic (or antiferromagnetic) properties are becoming increasingly important in view of their potential applications in sensor, actuation, and ferroelectric memory.[1–4] Meanwhile, they are promising materials in multiple-state memories, electric-field-controlled ferromagnetic resonance devices, and transducers with magnetically modulated piezoelectricity due to the magnetoelectric effect.[5–7] However, materials of this kind are very rare, as the two contrasting order parameters of ferroelectricity and magnetism are mutually exclusive.[2,3] Besides, most of them reveal multiferroic properties far below room temperature. So far, $BiFeO_3$ is the only one that exhibits multiferroism at room temperature with its Curie and Néel temperature of 1103 K and 643 K, respectively. However, there are high leakage current, inhomogeneous magnetic spin structure, and weak magnetoelectric coupling in $BiFeO_3$,[8,9] which restrict its applications in devices. Hence, it is a great challenge to seek new multiferroic materials with strong magnetoelectric coupling at room temperature.

Furthermore, among multiferroics currently under investigation, rare-earth manganites have been extensively studied owing to their tendency toward a strong magnetoelectric coupling. Among them, R_EMnO_3-type oxides with R_E = Ho–Lu,[10,11] belonging to hexagonal manganites, possess *c*-axis-oriented hexagonal ferroelectricity owing to the disappearance of a mirror image on the *a*–*b* plane with a tilting of the MnO_5 bipyramid units in a polar $P6_3cm$ unit cell, including $YMnO_3$.[12,13] Note that $YMnO_3$ is considered to have another structure which is similar to R_EFeO_3, that is, nonferroelectric orthorhombic structure with the space group of *Pbnm*.[14] Similarly, R_EFeO_3 may also exhibit hexagonal structure with dramatic multiferroic properties.[15] The claim proved to be true. Hexagonal R_EFeO_3 can only be prepared by using methods other than conventional high-temperature solid state routes, for example solution-based precursor methods,[16] spray ICP,[17] or as an epitaxially-grown thin film.[18–20] Jeong *et al.*[18–20] first fabricated the hexagonal $YbFeO_3$, $LuFeO_3$, and $YFeO_3$ films epitaxially on Al_2O_3 (0001) substrate and testified the existence of ferroelectricity in these antiferromagnetic films. In $YFeO_3$ film, they attribute the electronic origin of this artificially imposed ferroelectricity to the asymmetric $Y4d_z^2$–$O2p_z$ orbital overlapping along the *c* axis of $P6_3cm$ over the T–M first Brillouin zone.[20] Even so, the origin of multiferroism in $YFeO_3$ is controversial as it suffers from an insufficient understanding on leakage current, ferroelectric and magnetic mechanism.

In this study, we prepare the $YFeO_3$ film on Si(111) substrate by sol-gel spin-coating method, and investigate its crystal structure, surface morphology, leakage current characteristics, and ferroelectric properties. Meanwhile, its domain structures and switchable behavior are identified by piezoresponse force microscopy (PFM) also. The experimental results show that the hexagonal $YFeO_3$ film exhibits ferroelectricity at room temperature.

*Project supported by the National Natural Science Foundation of China (Grant Nos. 61471301, 61078057, 51202195, and 511172183), the Research Fund for the Doctoral Program of Higher Education of China (Grant No. 20126102110045), and the NPU Foundation for Fundamental Research (Grant Nos. JC201155, JC201271, and JC20120246).

†Corresponding author. E-mail: chenchl@nwpu.edu.cn

© 2015 Chinese Physical Society and IOP Publishing Ltd

2. Experiment

The $YFeO_3$ film was prepared by a conventional sol-gel spin-coating method. In the preparation experiment, *n*-type (111) orientation silicon wafers with a resistivity of 8–10 Ω·cm are used as the starting substrates. $Fe(NO_3)_3{\cdot}9H_2O$ and $Y(NO_3)_3{\cdot}6H_2O$ were used as the raw materials and dissolved in ethylene glycol diethylether. The citric acid was added as the stabilizer to the solution subsequently, forming a solution mixture with 0.1 M $Fe(NO_3)_3$, 0.1 M $Y(NO_3)_3$, and 0.3 M citric acid. The solution was stirred for 3 h and then aged for 24 h at room temperature to yield a precursor solution. The precursor solution was dip-coated on Si substrate and then spun at 1500 rpm. The as-deposited film was dried in air at 453 K for 4 min. These steps were repeated five times. Finally, the film was pyrolyzed to evaporate the solvent and remove organic residuals at 723 K for 15 min and was sintered at 1223 K for 2 h in air. The film produced was approximately 160 nm thick, as measured by spectroscopic ellipsometry (SE, Spec EI-2000-VIS).

The structure was analyzed by x-ray diffraction (XRD, D/Max2550VB+/PC, Rigaku) with a thin-film attachment and a CuK_α x-ray source was used. The incidence angle was fixed at 1.5° during scanning to increase the diffracted x-ray intensity of the film. The surface morphology and local piezoelectric response were investigated by atomic force microscope (AFM, MFP-3D-SA, Asylum Research) equipped with dual AC resonance tracking piezoresponse force microscopy (DART-PFM).[21] Measurements were taken using a Pt-coated tip (AC240TM electri-levers from Olympus with cantilever length l of 240 μm, resonant frequency of 70 kHz, spring constant k of 2 $N{\cdot}m^{-1}$). Vertical PFM measurements were performed at 800 kHz. The tip approaches the surface vertically until the deflection set point is achieved. The deflection set point used was 0.8 V. The leakage current and ferroelectric hysteresis-loop measurements were tested with ferroelectric test systems (Precision LC, Radiant Technologies Inc, USA) at room temperature. Here, Ag was pasted on the surface as top electrodes.

3. Results and discussion

Figure 1 is the thin-film x-ray diffraction (XRD) pattern of the film deposited on Si(111) substrate. The main characteristic peaks corresponding to (100), (101), (102), and (106) planes of the hexagonal perovskite $YFeO_3$ film were observed at about 28.8°, 29.6°, 32.2°, and 55.4°, respectively, which exhibits the polycrystalline nature of the $YFeO_3$ film. The peaks deviate slightly from the standard pattern due to the lattice mismatch between $YFeO_3$ film and Si substrate. Besides, some Fe_2O_3 impurity was observed (marked with $*$), which does not show ferroelectric property.

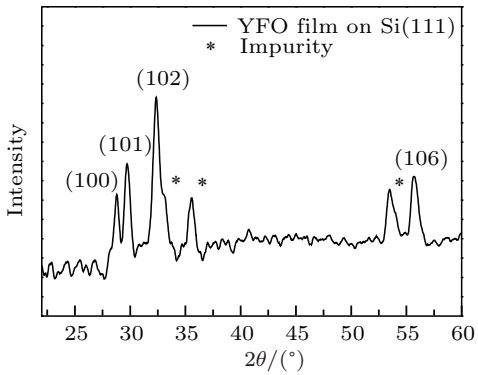


Fig. 1. XRD pattern of the $YFeO_3$ film on Si(111) substrates.

Typical current density (J) versus applied voltage (V) curve was measured from the Ag/$YFeO_3$/Si capacitor to study the leakage current behavior. Figure 2(b) shows the schematic of the test structure. Figure 2(a) shows that the J–V curve is substantially symmetric at low electric field and it becomes slightly different at high electric field. The maximal leakage current density under 5 V is about 5.4×10^{-6} A/cm^2. It is speculated that the leakage current of pure $YFeO_3$ will be lower. As is well known, the impurity in thin film can influence its electrical properties notably. It has been reported that in $BiFeO_3$,[22] the second phase Fe_2O_3 originated from the non-stoichiometry is responsible for the high leakage of $BiFeO_3$, as it has lower resistivity and can constitute percolating conduction paths and other defects, e.g., at the interfaces between $BiFeO_3$ and Fe_2O_3.

The J–V characteristics of the ferroelectric film are to regard contributions from conductance itself and interfacial conductance between film and electrode. Five conduction mechanisms in ferroelectric oxide thin films were commonly considered, namely, thermal electric conduction, Schottky emission, space-charge-limited conduction, Poole–Frenkel emission, and Fowler–Nordheim tunneling.[21,23] Figures 2(c) and 2(d) show the dependence of $\log(J)$ on $\log(V)$ at positive and negative bias, respectively. As can be seen, the plots are linear at lower voltage. The thick solid lines are the linear fit and the slopes are both close to 1, indicating the normal Ohmic contact behavior. That is to say, the leakage current is dominated by thermal electric conduction itself. While at higher voltage above 4 V, $\log(J)$ versus $\log(V)$ plots have the slopes of 1.36 and 1.26, which agree well with space-charge-limited current (SCLC) theory. Thus, the mechanism of the leakage current of the $YFeO_3$/Si interface obeys an Ohmic behavior and then changes to an SCLC behavior by increasing the bias. This mechanism is similar to that of $YMnO_3$/*n*-Si interface reported by Parashar *et al.*[23] Note that, the abrupt increase of the slope (> 2.64) occurs when the negative bias further increases (see inset in Fig. 2(d)) which could be explained by the FN tunneling model, indicating that the capacitor could be easy to breakdown after the SCLC process.

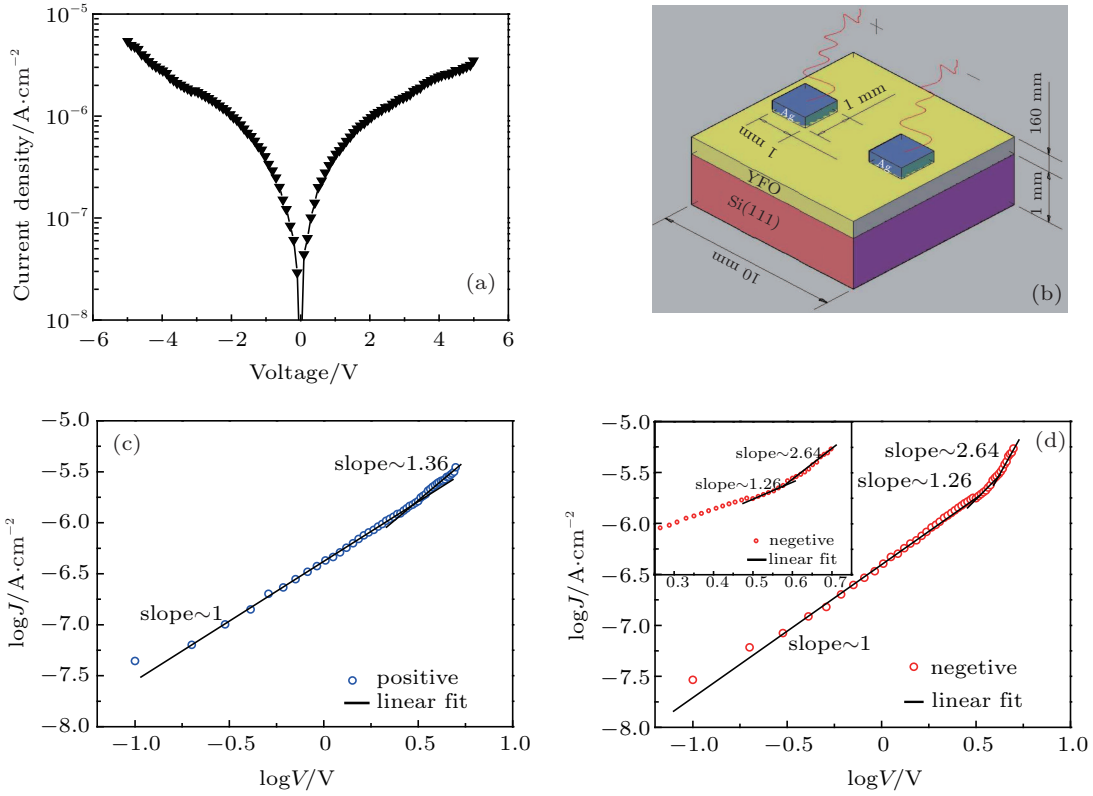


Fig. 2. (color online) (a) J–V curve of the Ag/$YFeO_3$/Si capacity, (b) schematic representation of capacity structure, (c) logarithm of the current density versus the logarithm of the voltage at positive bias, (d) logarithm of the current versus the logarithm of the voltage at negative bias.

The hysteresis loops of the $YFeO_3$ film were measured at room temperature, subsequently. As presented in Figs. 3(a) and 3(b), the $YFeO_3$ film reveals ferroelectric characteristics. It can be seen that the polarization is weak with small remnant polarization and coercive field, which is similar to that of the hexagonal $YFeO_3$ epitaxial film by PLD method.[19] Figure 3(a) shows the hysteresis curves at a frequency of 2 kHz under various applied electric fields. With the increase of electric fields, the polarizations increase accordingly. Under an applied electric field of 560 kV/cm, the remnant polarization (P_r) is about 0.07 μC/cm^2 and the coercive field (E_c) is 100 kV/cm. The loops at different frequency were plotted in Fig. 3(b). It can be seen that polarization of the film is slightly different and the P_r value under low frequency is larger than that under high frequency. In general, polarization charges of ferroelectric contribute not only from intrinsic polarization, space charges which come from the substrate–film or film–electrode interfaces play a significant role as well. The space charge effect became indistinct with the increase of frequency, which induces the decrease of P_r under high frequency. Note that we could not obtain the saturated polarization (P_s) as the hysteresis loop became rounded under higher electric field (not shown here). A major problem encountered is that its ferroelectric property is hampered by its leakage behavior, related to impurity Fe_2O_3, boundaries, etc.

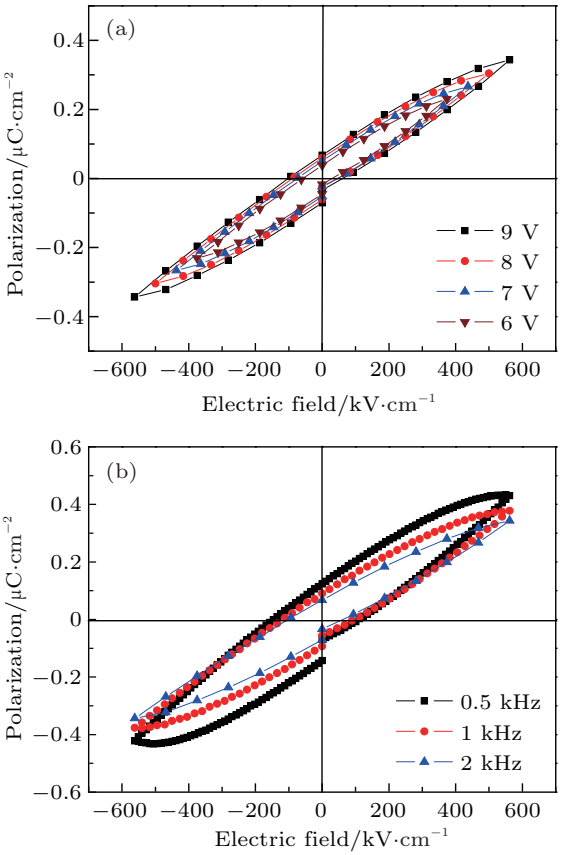


Fig. 3. (color online) (a) P–E ferroelectric hysteresis loops of the $YFeO_3$ film under various applied electric fields, (b) P–E ferroelectric hysteresis loops of the $YFeO_3$ film under different frequencies.

To further elucidate the ferroelectric properties of the $YFeO_3$ film, the topography and corresponding vertical piezoresponse images were captured by the standard PFM setup, as shown in Figs. 4(a)–4(c). It can be seen from the topographic image that the film presents granular microstructure with good connectivity at the surface. $YFeO_3$ grains are irregular spherical in shape with some deformation and the average grain size is less than 100 nm. The corresponding root-mean-square roughness (R_{RMS}) measured at the surface evaluating surface roughness is about 15.8 nm. Such grains are characteristic of three-dimensional island growth (Volmer–Weber mode).

The amplitude image (Fig. 4(b)) provides the magnitude of the piezoelectric coefficient along the normal direction while the phase image (Fig. 4(c)) provides a great deal of information about the direction of polarization in the domains.[24] The PFM phase image reveals a clear piezoelectric contrast associated with the direction of the polarization, with bright (yellow) and dark (violet) contrasts. Bright contrast indicates that the polarization of the domain is upward and perpendicular to the surface, and dark contrast corresponds to downward polarization. Obviously, the upward and downward domains are almost 180° apart. Besides, gray (orange) contrast occurs also, indicating the weak vertical piezoresponse signal. The gray constrast can be attributed to the following two aspects. First, it is a polycrystalline film and its grains show various orientations, so there may be domains with the polarization vector deviating from the direction normal to the film plane. According to Zeng,[25] different grain orientations of the film can result in the gray domain contrast. Second, the non-ferroelectric structure should be taken into account, based on the XRD data that reveal that the film contains the second phase of Fe_2O_3. Comparing PFM images simultaneously acquired with the topographic image, we find that it is not the one-to-one correlation between topographic and piezoresponse signals. A bright or dark contrast can belong to two or more grains, which means that grain boundary may not act as barriers for the domain-well motion.

Meanwhile, we measure the local amplitude and phase response loops under DC bias with a triangular waveform at a point in the desired domain regions, as shown in Fig. 4(d). A well-defined hysteresis phase loop as well as a butterfly-shape amplitude loop was observed, indicating the ferroelectricity in the $YFeO_3$ film further. The phase changes almost 180° (from 60° to 240°), which implies a nearly complete polarization switching behavior.

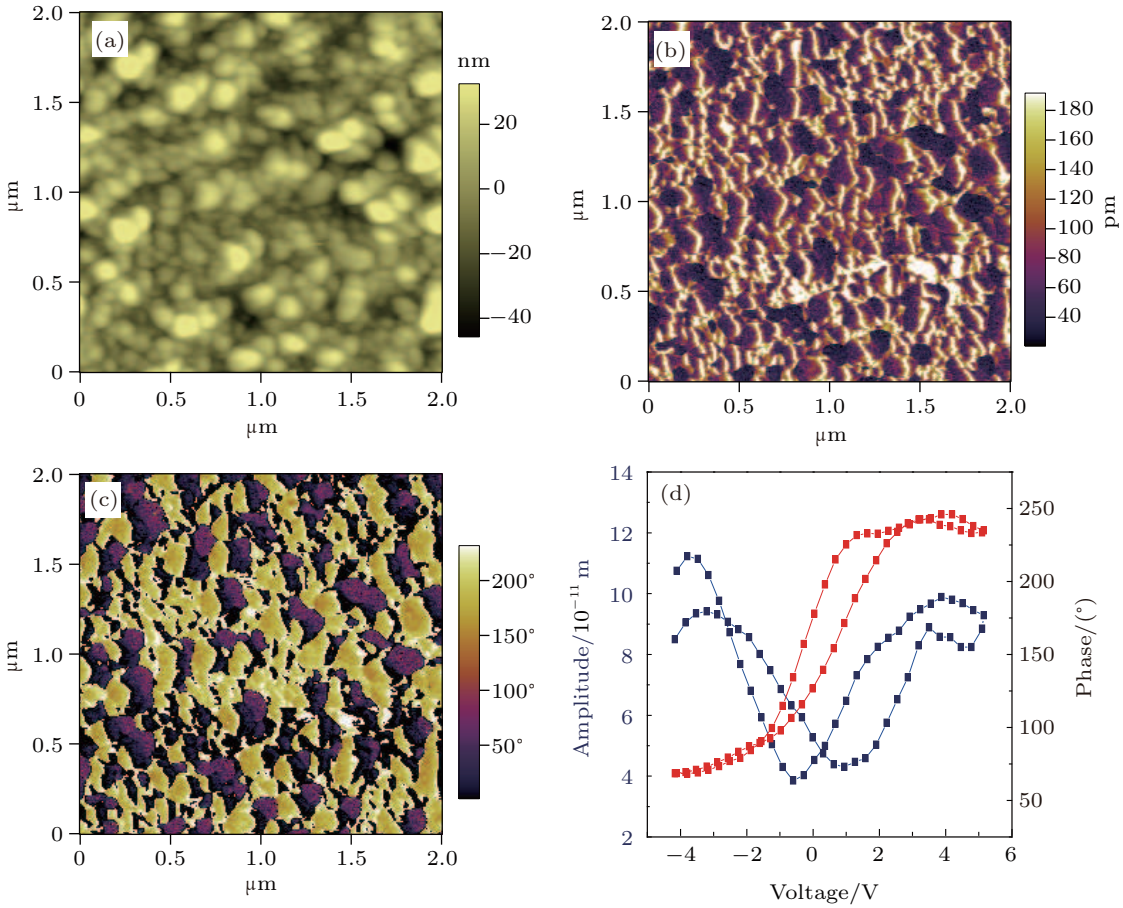


Fig. 4. (color online) PFM images of the ferroelectric domain structure of the $YFeO_3$ thin film deposited on Si(111) substrate over the scanning size of 2 μm×2 μm. (a) Topography image, (b) out-of-plane PFM amplitude image, (c) out-of-plane PFM phase image, (d) local amplitude loop and phase loop.

Note that the asymmetric loops were observed. The amplitude loop as well as the phase loop is simultaneously shifted toward the positive voltage. Similar results have been reported elsewhere.[26] The shift S value is 0.17 V, where S is defined as $S = (V_c^+ + V_c^-)/2$, with the right (V_c^+) and left (V_c^-) hand coercive voltage, respectively. This slight shift is caused partly by the asymmetry of the tip/film/bottom electrode. Secondly, the shift is considered as the evidence of the internal field by trapped space charges.[27,28] The asymmetric behavior suggests that the phase reversal phenomenon in the vertical phase images results not from the buckling effect of shear mode, but from the relaxation effect of ferroelectric domains.[29]

4. Conclusions

In summary, $YFeO_3$ film about 160 nm with hexagonal structure was prepared on Si(111) substrate by sol–gel synthesis method. The leakage current density of the $YFeO_3$ film is 5.4×10^{-6} A/cm^2 at a drive voltage of 5 V and shows good characteristics for practical applications. Three different regions, i.e., Ohmic contact, SCLC, and FN tunneling were observed in J–V characteristics. The P–E hysteresis loops at room temperature demonstrated ferroelectricity of the $YFeO_3$ film. Owing to the high leakage induced by the impurity of Fe_2O_3, the saturated polarization was not observed. Nanoscale domain structure and its reversal behavior of the film were also investigated by the PFM techniques, which further evidenced the polarization behavior of the $YFeO_3$ film. The slight shift of the amplitude loop and phase loop to positive voltage is caused by the asymmetry of the electrode and the interfacial-induced charges. The present work strongly promotes the need for better understanding of the multiferroism in the hexagonal ferrite film.

References

[1] Catalan G and Scott J F 2009 *Adv. Mater.* **21** 2463
[2] Cheong S W and Mostovoy M 2007 *Nat. Mater.* **6** 13
[3] Hill N A 2000 *J. Phys. Chem. B* **104** 6694
[4] Lin Y H, Ying M, Li M, Wang X and Nan C W 2007 *Appl. Phys. Lett.* **90** 222110
[5] Bi K, Wu W and Wang Y G 2011 *Chin. Phys. B* **20** 067503
[6] Song Y Q, Zhou W P, Fang Y, Yang Y T, Wang L Y, Wang D H and Du Y W 2014 *Chin. Phys. B* **23** 077505
[7] Wu T, Emmons M, Chung T K, Sorge J and Carman G P 2010 *J. Appl. Phys.* **107** 09D912
[8] Qi X D, Dho J, Tomov R, Blamire M G and MacManus-Driscoll J L 2005 *Appl. Phys. Lett.* **86** 062903
[9] Lin P T, Li X, Zhang L, Yin J H, Cheng X W, Wang Z H, Wu Y C and Wu G H 2014 *Chin. Phys. B* **23** 047701
[10] Jeong Y K, Lee J H, Ahn S J, Song S W, Jang H M, Choi H and Scott J F 2012 *J. Am. Chem. Soc.* **134** 1450
[11] Van-Aken B B, Palstra T T M, Filippetti A and Spaldin N A 2004 *Nat. Mater.* **3** 164
[12] Talbayev D, LaForge A D, Trugman S A, Hur N, Taylor A J, Averitt R D and Basov D N 2008 *Phys. Rev. Lett.* **101** 247601
[13] Gibbs A S, Knight K S and Lightfoot P 2011 *Phys. Rev. B* **83** 094111
[14] Mathur S, Veith M, Rapalaviciute R, Shen H, Goya G F, Martins-Filho W L and Berquo T S 2004 *Chem. Mat.* **16** 1906
[15] Downie L J, Goff R J, Kockelmann W, Forder S D, Parker J E, Morrison F D and Lightfoot P 2012 *J. Solid State Chem.* **190** 52
[16] Li J, Singh U G, Schladt T D, Stalick J K, Scott S L and Seshadri R 2008 *Chem. Mat.* **20** 6567
[17] Mizoguchi Y, Onodera H, Yamauchi H, Kagawa M, Syono Y and Hirai T 1996 *Mat. Sci. Eng. A* **218** 164
[18] Jeong Y K, Lee J H, Ahn S J and Jang H M 2012 *Chem. Mat.* **24** 2426
[19] Ahn S J, Lee J H, Jeong Y K, Na E H, Koo Y M and Jang H M 2013 *Mater. Chem. Phys.* **138** 929
[20] Oak M A, Lee J H and Jang H M 2011 *Phys. Rev. B* **84** 153106
[21] Luo B C, Wang D Y, Duan M M and Li S 2013 *Appl. Surf. Sci.* **270** 377
[22] Lahmar A, Zhao K, Habouti S, Dietze M, Solterbeck C H and Es-Souni M 2011 *Solid State Ionics* **202** 1
[23] Parashar S, Raju A R, Rao C N R, Victor P and Krupanidhi S B 2003 *J. Phys. D: Appl. Phys.* **36** 2134
[24] Fan F, Luo B C, Duan M M and Chen C L 2013 *Chin. J. Phys.* **51** 834
[25] Zeng H R, Li G R, Yin Q R and Xu Z K 2003 *Mater. Sci. Eng. B* **99** 234
[26] Zhang R L, Chen C L, Duan M M, Niu L W and Jin K X 2014 *J. Crystal Growth* **390** 56
[27] Gruverman A, Rodriguez B J, Nemanich R J and Kingon A I 2002 *J. Appl. Phys.* **92** 2734
[28] Ferri A, Saitzek S, Da Costa A, Desfeux R, Leclerc G, Bouregba R and Poullain G 2008 *Surf. Sci.* **602** 1987
[29] Jang Y H, Kim C H, Seo S J and Cho J H 2013 *Thin Solid Film.* **548** 52